Creep Properties of Intact and Fractured Muddy Siltstone

O. Hamza
College of Engineering and Technology, University of Derby, Markeaton Street, Derby DE22 3AW, UK
Corresponding author: o.hamza@derby.ac.uk

R. Stace
Department of Civil Engineering, Faculty of Engineering, University of Nottingham, Nottingham, UK

ABSTRACT

Time-dependent characterisation of rocks for the entire strain range (i.e. up to and beyond the yield point, where rocks are expected to be fractured) have received considerable attention for improving the long-term stability of deep underground openings. Although extensive experimental studies have been carried out on creep of different types of rocks, very limited studies exist, which investigate intact as well as fractured rock samples taken from the same type of rock.

In this paper, the time-dependent behaviour of muddy siltstone was investigated to determine and compare creep properties of intact and fractured rock samples. A series of multistage uniaxial and triaxial creep tests were conducted on the rock samples at room temperature. In addition, multistage triaxial testing was conducted on the rock (intact and fractured) to determine the instantaneous (short-term) stiffness and explore its correlation with creep properties.

All stain curves showed an initial instantaneous strain followed by two phases of time-dependent strain including transient creep phase (particularly for the first loading stage) and a steady state creep phase. The results indicate that both the instantaneous and creep strain are proportional to the deviatoric stress and confining pressure. This is clearly evident in the fractured rock samples, where larger deviatoric stress resulted in an increased creep strain and strain rate.

The relationship between axial strain and time was successfully fitted to Burgers creep model. In comparison with the intact rock, creep parameters (of the Burgers model) for the fractured rock were found to be significantly smaller, corresponding to the larger creep deformation and steady-state creep rate experienced by the fractured rock samples. Despite this difference between the intact and fractured rock samples, the study showed a considerable correlation between the creep parameters of both types of rock samples and their instantaneous elastic modulus (obtained at typical confining pressures). Regression analysis revealed that creep parameters could be reasonably estimated from instantaneous elastic modulus using an exponential function.

Furthermore, based on the experimental findings, an improved characterisation of time-dependent properties was proposed. We believe this approach provides a good basis for future

research to enhance geotechnical modelling of long-term stability of abandoned mines as well as for the application of underground disposal of radioactive waste and oil and gas storage.

Keywords:
Time-dependent deformation, Creep test, Fractured rock, Burgers model

1 Introduction

In deep underground excavation, rock mass response may be classified as time-*in*dependent or time-dependent and the material (whether it is intact or fractured) may behave elastically or may yield according to the applied stress level[1]. An understanding of the time-dependent behaviour has been considered essential for further development in the field of underground mine design and long-term strata control[2], and more recently it has become important for the application of underground disposal of radioactive waste[3–5].

It is generally believed in coal mines that after the initial excavation of an entry, most coal-measure rocks show time-dependent deformation, even when no activity is taking place nearby[6]. This deformation usually appears in different forms[7,8] such as roof sag, floor heave, pillar dilation, or shearing along bedding planes and joints. This rheological deformation might be followed by 'disturbance deformation', which is caused by stress changes due to mining activities in adjacent areas[9]. These physical events (observed in underground excavation) have been attributed to time-dependent characteristics, which can also be measured in a small rock sample tested in laboratory.

Conventional laboratory experiments have used three testing methods to investigate time-dependent behaviour; these are: (i) creep, (ii) relaxation and (iii) loading tests at different stress or strain rates. Creep in particular can be observed in laboratory testing when *relatively high* stress is constantly applied on a cylindrical specimen over a period of time. Fig. 1 shows an idealised creep curve which exhibits three out of four principal phases of deformations as listed below:

a) Instantaneous elastic strain due to instantaneous load.
b) Primary or transient creep with rapid strain increments, however at a decelerating strain rate.
c) Secondary creep at low, or near constant strain rate.
d) Possible tertiary creep accelerating strain increment to failure, which might take much longer time than in the lab studies[10].

If the specimen is unloaded during the primary creep stage, the deformation can be recovered. However, permanent deformation is resulted if the secondary creep is dominated. To represent such time-dependent behaviour of rocks in mathematical form, mechanical, phenomenological or rheological models are commonly developed by fitting the experimental data[11,12] on the basis of empirically observed internal variables[13] or the superposition of several vicious and elastic elements such as the Burgers body model[14].

Extensive creep testing has been conducted on coal-measure rocks around the mid of last century. In early stages (prior to 1964), the majority of the time-strain experiments have been carried out in uniaxial compression, at room temperature and, for periods of less than a week[15–18]. These studies have been mostly carried out on intact rock samples. However, the time-dependent behaviour of fractured rock represents an important condition of rock mass. Larson and Wade[19] indicated that creep in brittle coal measure rock occurs, likely, because of (i) micro-

cracking along weak bedding planes and (ii) weakening of asperities of joints. Therefore creep along bedding plan and pre-existed joints is also important. This has been investigated in a number of studies as explained below.

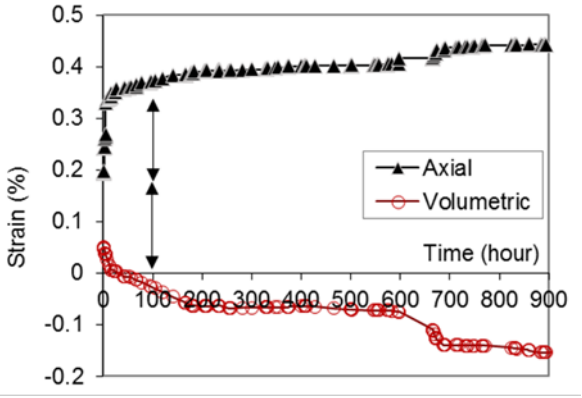

Fig. 1. Axial and volumetric strain curves for Lea Hall Sandstone under 35.8 MPa uniaxial stress showing three stages of creep (after Hobbs, 1970).

Höwing and Kutter[20] conducted direct-shear tests to investigate the effects of joint filler on creep behaviour. In this study, creep velocity during the primary phase has followed a power law, up to the point where creep progressed from the primary to the tertiary phase.

Clean joints have been investigated in uniaxial and triaxial compression tests on intact and jointed rock specimens of Westerly Granite and Navaho Sandstone[21]. The study has shown that creep behaviour of jointed rock has a similar character as that of the intact material, but with a larger amount of strain. Larson and Wade[19] investigated friction and creep characteristics of weak planes in mudstone by conducting direct-shear creep tests; non-linear rheological model[22] has been used to fit their experimental data.

More recently, a microcrack-based damage constitutive law, established at the elemental scale, has been used to directly link the time-dependent degradation of elastic stiffness and the induced anisotropy to microcrack propagation[23]. Although this model is an attractive solution to reproduce the macroscopic creep behaviour on the basis of the microscopic kinetics of microcrack growth, the model requires proper calibration in order to obtain reliable results. Therefore, it appears that phenomenological and empirical approaches might still be good alternative ways and therefore they were adopted in this study to characterise and compare the rheological behaviour of all rock samples tested.

Although extensive research has been conducted on creep of intact as well as jointed rocks, very limited studies exist which investigate both conditions for the same type of rock. In a previous laboratory work[24], it has been found that the effect of strain rate on broken rock samples can be significantly greater than that of the intact rock samples (depending on the confinement), indicating that the ability of rock to relax or creep considerably increases in fractured rocks. Despite this difference, a similar phenomenological model has been successfully used[24] to represent the effect of strain rate on strength and stiffness of both intact and fractured silty mudstone. It follows that other time-dependent behaviours such as creep can be modelled for both intact and fractured rock using a similar phenomenological approach such as the Burgers creep model. Furthermore, the creep model parameters might have a certain pattern of correlation between the intact and fractured rocks. These aspects were investigated

in this paper using laboratory experiments conducted on small-scale samples of intact and fractured muddy siltstone. The study can improve our understanding of the rheological properties of argillaceous rocks particularly at pre and post-failure conditions generated by mining activities; it also provides a good basis to enhance geotechnical modelling of long-term stability of deep underground openings, which is significant for many engineering applications such as mining and petroleum engineering, and safety assessment of radioactive waste disposal.

2 Experimental method

2.1 Materials and Apparatus

The rock material selected for the laboratory experiments was obtained from an open pit mine located at Arkwright in the Midlands of the UK. The recovered rock consists of laminated muddy siltstone (also described as silty mudstone in places) which is grey in colour with darker bands. The rock has a dry density of 2.48 ± 0.01 g/cm^3 and specific gravity of approximately 2.75.

To reduce any possible variability in the mechanical properties, the samples were cored from carefully selected similar blocks, which were mostly dominated by a similar angle of lamination (i.e. 0^o-7^o to the horizon of specimen flat surface). After coring, the rock samples were left to dry out for 24 hours at 100^{o}C and then coated with a very thin layer of flexible varnish to eliminate the effect of humidity so that the unweathered condition of the material would be maintained over the storing and testing periods.

The tests were conducted at room temperature (20±1.5^{o}C) on cylindrical dry samples of 74mm in height and 36mm in diameter, which were prepared following the procedures outlined by ISRM (1981). A total of 14 out of 16 samples of the muddy siltstone were successfully tested and reported in this paper.

Before conducting the creep experiments, six samples were initially tested to obtain the instantaneous strength and stiffness of the intact and fractured rock at different confining pressures. The experiments were conducted using uniaxial compression test as well as multistage triaxial testing technique (MSTT). The MSTT technique enables experimenters to conserve samples and to obtain more consistent strength and stiffness data by eliminating sample variability. Loading on samples was carried out at a strain rate equal to approximately 10^{-5} s^{-1}.

The remaining eight rock samples (i.e. four intact and four fractured) were used for creep tests conducted under uniaxial and multistage triaxial loading conditions, where a constant axial stress σ_1 was applied and maintained by a servo-controlled rig machine. The equipment is perfectly suitable for conducting uniaxial creep compression tests; however, the required triaxial loading condition was achieved by confining the sample using a Hoek cell connected to a manual pump. This equipment can maintain constant confining pressure throughout the test. The axial displacement was measured by a high precision displacement gauge, and the recorded deformation was corrected for the stress effect on the steel Platens used for the application of axial stress.

The fractured rock samples were produced from the intact rock samples after bringing them to failure in conventional triaxial compression tests. A similar pattern of fractures was noticed in which rock samples developed a major shear plane at about 45^o from horizontal. It is important to clarify that the fractures considered in the study are limited to shear failure surface generated by compression effect. A future study might be conducted on rock fractures generated by tensile failure.

After creating the failed (fractured) specimens, they were then used to carry out multistage creep testing with the prescribed confining pressure σ_3 (ranging between 1 and 6 MPa). Larger values of confining pressure would have allowed a better investigation of the triaxial creep behaviour. However, the chosen range was based on the best performance of the equipment used in the experimental programme.

2.2 Secondary creep strain

Secondary or Steady State (SS) creep strain rate (see Fig. 1) is an important parameter and several research studies[11,25–27] conducted over a number of rocks and hard soils have shown that the steady-state creep strains are almost independent of the loading history and are a function of the current stress state only. For many engineering applications, it is essential to know when a steady state (SS) condition is reached and what magnitude it can be at a certain level of stress.

This was investigated at an early stage of our experimental programme to determine the likely timescale required to obtain steady-state creep for the intact muddy siltstone. Fig. 2 shows a typical creep curve conducted at constant axial stress σ_1= 32 MPa (≈57% of UCS); as expected the secondary creep did not start before some time i.e. approximately 1200 minutes (less than one day). Previous research[26,28] conducted on rock salt has shown that time required to reach SS strain increases as deviatoric stress increases. Therefore, in planning for our experiments, the rock samples were given approximately two days to creep for each stress increment (stage). This procedure was found to be adequate to allow the steady state (SS) strain rate to be obtained, which is of great importance for modelling and characterising time-dependent behaviour.

Throughout the experimental programme, tertiary creep was not encountered within the timescale given for the rock samples to creep. Therefore, tertiary creep is out of the scope of this study.

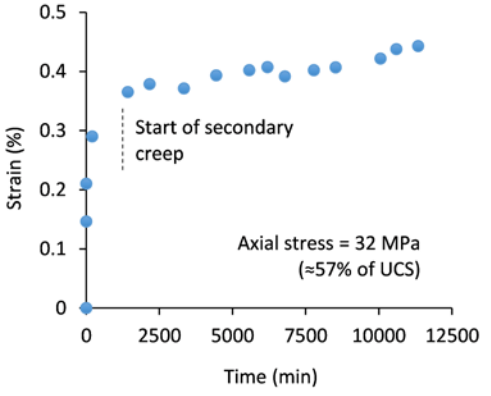

Fig. 2. Uniaxial creep test showing the period required to obtain secondary creep in an intact muddy siltstone sample under an axial stress of 32 MPa.

3 Results and discussion

3.1 Instantaneous (short-term) strength and stiffness

Prior to conducting any creep experiment, six samples were initially tested to determine the instantaneous strength and stiffness of the intact and fractured rock samples of the muddy siltstone. Fig. 3-b shows experimental results from a selected test conducted on an intact sample at different confining pressure (σ_3) ranging from 2 to 6 MPa. The axial stress-strain data in each stage was precisely fitted to the 6th order of a polynomial function and then the derivative, which represents the tangent modulus of elasticity (E_t), was obtained.

The tangent modulus of elasticity (E_t) represents the slope of the stress-strain curve at any point. The fluctuation of this modulus throughout the multistage is shown in Fig. 3-b: in the first stage, E initially increased in magnitude until reaching a peak value (e.g. elastic-limit), where the material would be expected subsequently to deform plastically. Proceeding to the next stage by increasing the confining pressure, the tangent modulus E_t showed a jump and then typically decreased as if the material was continuing the yielding phase (inelastic deformation). For the analysis, the peak strength (σ_p) was taken as the maximum axial stress applied in each stage (Fig. 3-a), and the elastic modulus E in each stage was considered as the highest value of E_t (Fig. 3-b). This procedure for estimating E may be appropriate in the first stage; however E can be underestimated in the following stages because the sample is likely to have experienced some plastic deformation before the proceeding to the next stage. Nevertheless, the procedure permitted consistent estimation of stiffness between all samples, which was appropriate for the generic nature of this experimental study.

Summary of the results of these experiments is presented in Fig. 4, where the peak strength (σ_p) and the elastic modulus (E), including the standard deviation, are plotted at different confining pressures. From these results, it is interesting to note that in both the intact and fractured rock samples the effect of confinement on the elastic modulus (E) is clearly dominant, where E values increase with the confining pressure. A strong relationship between E and confining pressure has been reported in the literature[24,29]. A similar trend was observed for the rock peak strength properties as expected (Fig. 4).

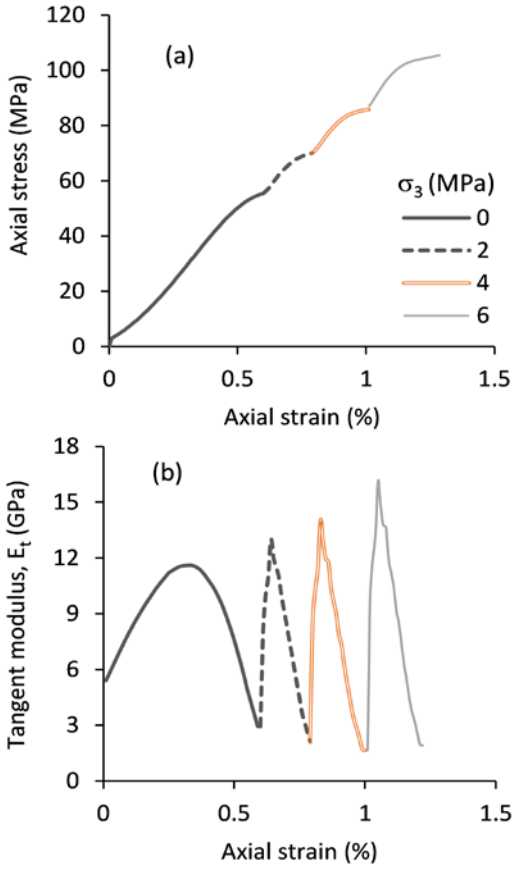

Fig. 3. Four-stage triaxial compression test conducted on an intact sample of muddy siltstone at different confining pressures (σ_3).

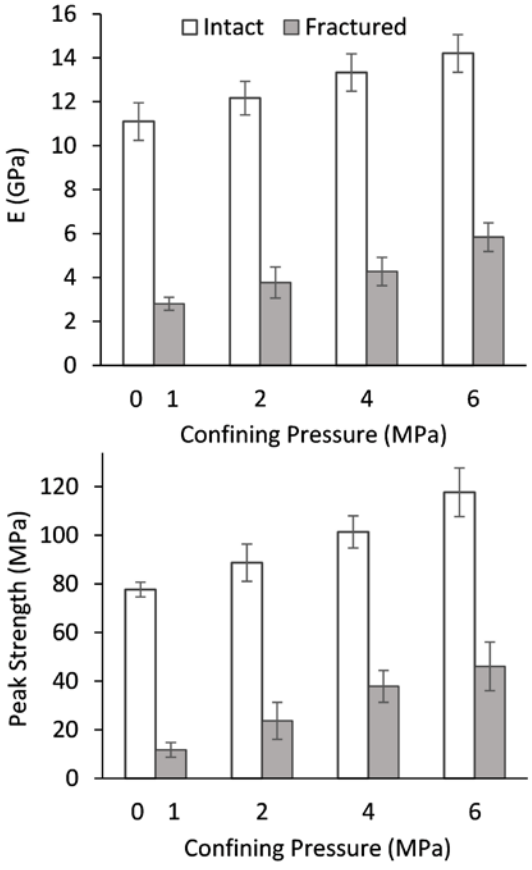

Fig. 4. Instantaneous properties: peak strength and elastic modulus of the intact and fractured rock samples.

3.2 **Creep experimental results on intact and fractured rock samples**

Fig. 5-a shows results of multistage creep tests conducted on four intact rock samples at four different confining pressure σ_3 (0, 2, 4, and 6 MPa). For each sample, a constant confining pressure was applied, while the axial stress was increased in three stages: σ_1= 31.2, 39.1, and 46.8MPa. These values are approximately equivalent to 40%, 50%, and 60% of the average instantaneous peak strength σ_p of the intact rock at confining pressure σ_3 = 2 MPa, respectively. Summary of stresses applied on the intact rock samples is presented in Table 1.

Table 1
Stresses used for multistage creep experiments on intact rock samples

Test ID		**Test 1**	**Test 2**	**Test 3**	**Test 4**
σ_3 (MPa)		0	2	4	6
$q = \sigma_1 - \sigma_3$	**Stage1**	31.1	29.3	27.2	25.2
	Stage2	39.1	37.1	35.2	33.1
	Stage3	46.8	44.7	42.8	40.6

Table 2 presents all stresses applied on the four fractured rock samples, where the following confining pressures (σ_3) were used: 1, 2, 4, and 6 MPa. Because of the loose structure of these samples, it was not possible to conduct the test without a minimum confinement of 1 MPa. The overall confinement values (σ_3) are within the same range applied on the intact samples. However smaller values of axial stress (σ_1) were applied on the fractured rock samples because these are much weaker than the intact rock samples (according to the instantaneous properties of both rocks). Four multistage creep tests were conducted on the fractured rock samples. In each test, the axial stress (σ_1) was increased in three stages: 10.35, 12.8, and 15.10 MPa. These values are approximately equivalent to 40%, 50%, and 60% of the average short-term peak strength of the fractured rock at confining pressure of 2MPa, respectively. The creep results of the fractured rock samples are shown in Fig. 5-b.

Table 2
Stresses used for multistage creep experiments on fractured rock samples

Test ID		**Test 1**	**Test 2**	**Test 3**	**Test 4**
σ_3 (MPa)		1*	2	4	6
$q = \sigma_1 - \sigma_3$	**Stage1**	9.35	7.39	5.36	3.37
	Stage2	11.8	9.7	7.6	5.7
	Stage3	14.10	12.04	10.08	8.04

* Sample is unstable when σ_3 is less than 1 MPa

3.3 **General observation on creep behaviour**

The most noticeable finding to emerge from the creep data is that all stain curves (Fig. 5-a and 5-b) showed an initial instantaneous strain followed by two phases of time-dependent strain including transient creep phase (particularly for the first loading stage) and a steady state creep

phase. Accelerated or tertiary creep was not considered in this study because the applied stresses were adequately less than the short-term compressive strength of the rocks.

The results also indicate that both the instantaneous and creep strain are proportional to the deviatoric stress. This is clearly evident in the fractured rock samples where larger deviatoric stress resulted in an increased creep strain and strain rate.

3.4 The effect of deviatoric and confining pressure on strain magnitude

The experiments conducted on intact rock samples show that the rock exhibits larger creep strain at larger deviatoric stress at almost similar rate regardless of confining pressure. Unlike the results from the fractured rock samples where the creep strain is not only proportional to deviatoric stress but also to the level of confining pressure, where the temptation for creep decreased with the increase of confinement. This is not clearly shown in the intact rock samples, possibly because of the low level of confining pressure (less than 6 MPa) in comparison with its high strength (UCS=56 MPa).

To further investigate the effect of confinement on creep behaviour of both the intact and fractured rock samples, an additional analysis was carried out, in which the cumulated strains recorded after approximately two days from the start of each loading stage are plotted against deviatoric stress, as shown in Fig. 6. From this figure, it is possible to assess the tendency of creep in relation to deviatoric stress for all rock samples. The intact rock showed an average value of 0.02% of creep strain per MPa, whereas the fractured rock presented larger variation: from 0.09 to 0.03% of creep strain per MPa for a confining pressure ranging from 1 to 6 MPa, respectively. This implies that creep tendency decreases with the increase of confining pressure.

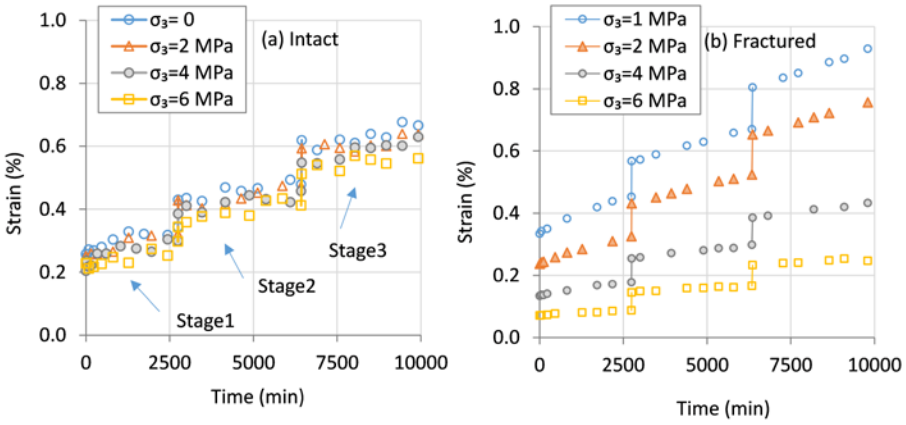

Fig. 5. Creep strain vs. time obtained from (a) four *intact* samples, and (b) four *fractured* samples of the muddy siltstone.

3.5 The effect of deviatoric and confining pressure on steady state (SS) strain rate

The effect of confining pressure and deviatoric stress on steady state (SS) creep rate was also investigated. For the intact rock, the SS creep rate was approximately 0.023% per day. By contrast, the fractured rock showed a specific trend, in which the SS creep rate decreased from approximately 0.05% to less than 0.01% per day (as illustrated in Fig. 7) in response to the increase in confining pressure from 1 to 6 MPa. This finding is in line with those of other previous studies[30] conducted on cataclastic rocks in a multi-loading triaxial creep test. The

relationship between the steady strain rate and deviatoric stress (for the fractured rock) was found to be best expressed by the following power-law function (see Fig. 8):

$$\varepsilon' = 10^{-7}\, q^{3.215} \quad (1)$$

where ε' = steady state (SS) strain rate measured in d^{-2} (d= day), and q is deviatoric stress in MPa.

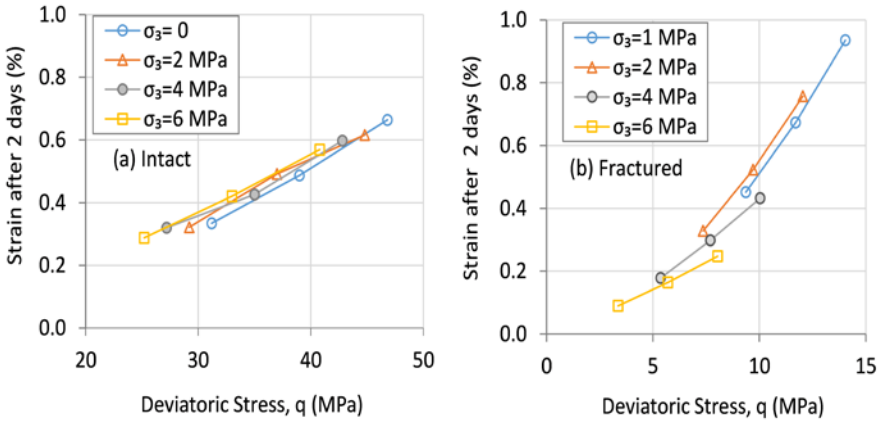

Fig. 6. Strain value (recorded after approximately two days from the start of each loading stage) plotted against deviatoric stress for: (a) Intact rock samples, (b) Fractured rock samples.

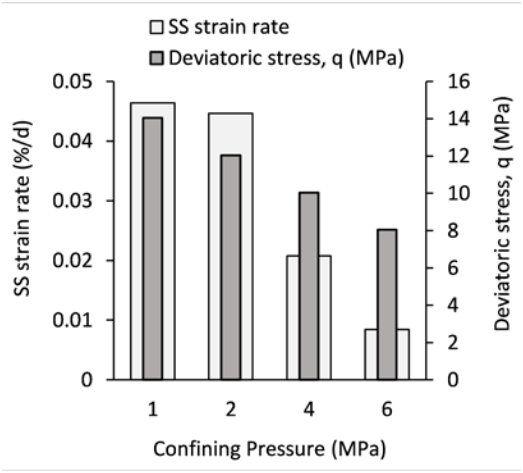

Fig. 7. The effect of confining pressure and deviatoric stress on steady state (SS) strain rate in the fractured rock samples.

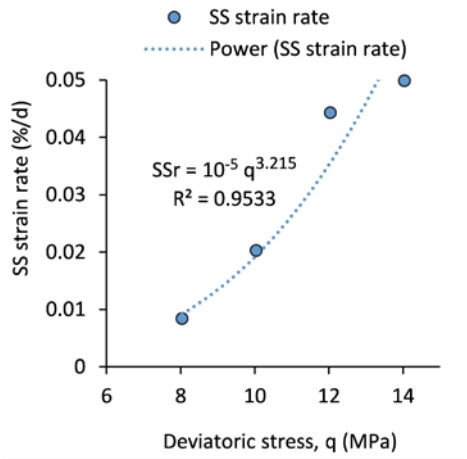

Fig. 8. Relationship between steady state (SS) strain rate and deviatoric stress for the fractured rock samples.

3.6 **Analysis of creep model**

Creep experimental data are usually analysed and fitted to the best mathematical expressions or *models*. These models with representative material properties are highly required to predict the geotechnical performance and also for the design applications. Many constitutive laws (models) considering the effect of time have been developed using (i) Experimental/empirical fitting, (ii) Mechanical models and (iii) Phenomenological models based on physical process theories.

Burgers model is one of the most successful constitutive laws that have been used to model creep behaviour of rocks[1,25,31–37]. Burgers model possesses instantaneous deformation

properties, the primary creep, and steady creep. The constitutive equation of this model can be expressed as:

$$\varepsilon = \sigma\left[\frac{1}{E_m} + \frac{t}{\eta_m} + \frac{1}{E_k}\left(1 - e^{-\frac{E_k t}{\eta_k}}\right)\right] \quad (2)$$

where ε = strain, σ = stress, t = time, and the rest are the model's parameters. In general, the parameters required for Burgers model are:

- Kelvin Parameters: Kelvin modulus (E_k) and Kelvin viscosity (η_k);
- Maxwell parameters: Maxwell modulus (E_m) and Maxwell viscosity (η_m).

In the current study, these parameters were determined through a non-linear, least squares regression analysis using Matlab (Mathworks). The values of parameters obtained for the creep tests are presented in Table 3. The model was found to be suitable to describe the experimental data with good accuracy (R^2 = 0.87 - 0.93).

Table 3
Creep parameters of the intact and fractured rock samples under different confining pressures

σ_3 (MPa)	E_m (GPa)	η_m (GPa.d)	E_k (GPa)	η_k (GPa.d)
Intact				
0	11.2	150.3	50.1	50.4
2	11.9	162.4	52.3	52.2
4	12.5	171.5	49.8	53.1
6	13.4	169.8	58.4	52.9
Fractured				
1	2.8	60.5	15.2	23.3
2	3.1	72.4	16.0	23.1
4	4.0	94.8	19.6	28.9
6	4.5	101.4	30.2	30.6

The values of Table 3 are presented in Fig. 9, where the parameters are plotted against the confining pressures. This suggests that the fractured rock has generally smaller creep parameters (smaller stiffness), thus allowing much larger magnitude of creep deformation in comparison with the intact rock. These factors may explain the relatively good correlation between strength and stiffness of several rocks and their tendency for creep as previously reported by several authors[25,33].

In Burgers model, Maxwell parameters illustrate the property of secondary creep (i.e. the creep exhibited by this model is non-recoverable), while the Kelvin parameters exhibit the property of primary creep, which is recoverable upon removal of the stress field[33]. For all tested samples, Maxwell viscosity (η_m) was found to be generally much larger than Kelvin viscosity (η_k), however Maxwell modulus (E_m) was smaller than Kelvin modulus (E_k).

Another significant finding revealed in Fig. 9 is that the confining pressure has a different effect on creep parameters. The effect is clearer in the fractured rock where the creep parameters generally increase with the increase of confinement. Further investigation of these variables for a wider range of confinement and deviatoric stresses, will be carried out in future studies.

3.7 **Relationship between instantaneous and creep parameters**

As both the (short-term) instantaneous and creep properties were found to be a function of confining pressure, it may be the case therefore that creep properties can be normalised by the instantaneous elastic modulus (E) obtained at the same confinement. The normalised creep parameters are calculated and illustrated in Fig. 10. The figure indicates the significant reduction in the difference in creep properties between the intact and the fractured rock based on normalisation (as illustrated in Fig. 9). This finding poses a substantial implication for estimating time-dependent properties of rocks based on their instantaneous properties.

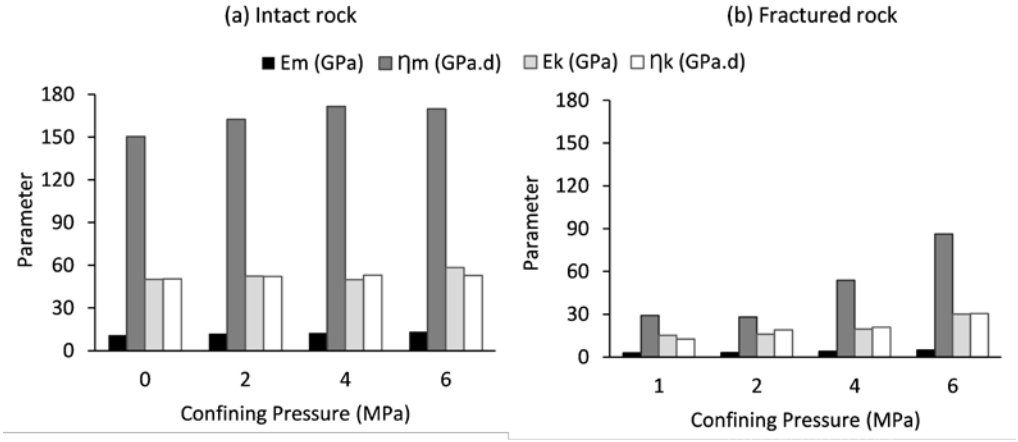

Fig. 9. Parameters of Burgers model at different confining pressures: (a) Intact rock samples, (b) Fractured rock samples.

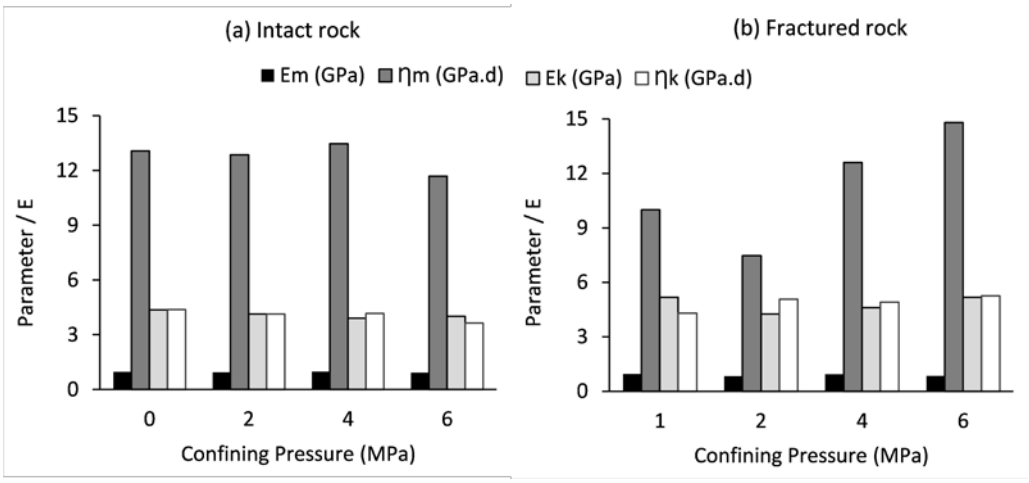

Fig. 10. Parameters of Burgers model normalised by the elastic modulus, E: (a) Intact rock samples, (b) Fractured rock samples.

Furthermore, the relationship between Burgers parameters and short-term elastic modulus (E) can be described by an exponential function. For a given elastic modulus (E), the Burgers parameters (y) may be calculated for the intact and fractured muddy siltstone from the following equation:

$$y = A\, e^{B.E} \qquad (3)$$

where *A* and *B* values are given in Table 4.

Table 4
Values of constants *A* and *B* in Equation 3

	E_m (GPa)	η_m (GPa.d)	E_k (GPa)	η_k (GPa.d)
Intact				
A	5.5642	101.87	26.63	43.345
B	0.0611	0.0367	0.0529	0.0144
R^2	0.9288	0.5868	0.8077	0.5748
Fractured				
A	1.5579	7.957	6.8165	5.8151
B	0.2002	0.4083	0.2501	0.2918
R^2	0.9336	0.8651	0.9537	0.9551

The corresponding fitted curves and other Burgers parameters in relation to the short-term elastic modulus (E) are shown in Fig. 11. The figure indicates that the creep parameters are all fitted the proposed exponential function very well except the viscosity parameters (η_m, η_k) of the intact rock, where least-squares (R^2) is less than 0.6.

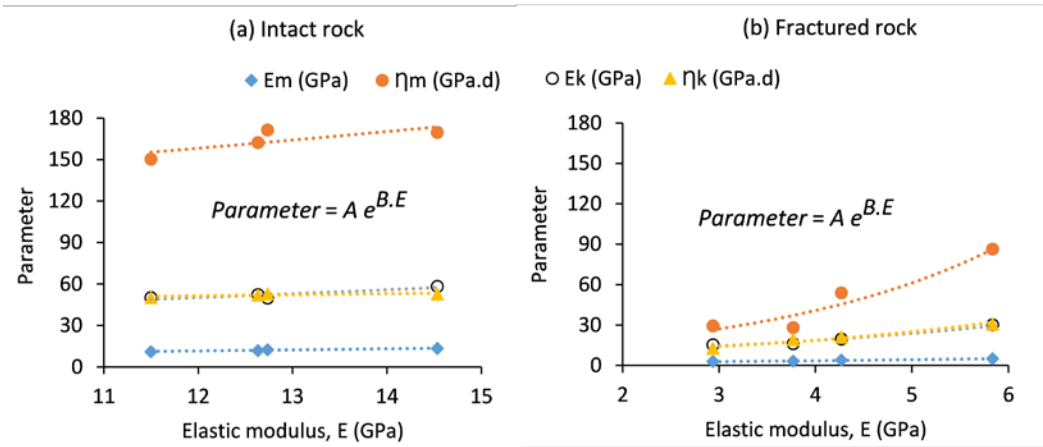

Fig. 11. The exponential relationship between Burgers parameters and short-term elastic modulus (E): (a) Intact rock samples, (b) Fractured rock samples.

4 Conclusion

The main goal of this study is to investigate the creep behaviour of muddy siltstone under axial and triaxial stresses and compare the time-dependent properties of intact and fractured rock samples, which may represent two *generic* ultimate conditions of rock mass (pre and post failure). The study has also explored the relationship between the instantaneous (short-term) stiffness and creep properties.

Within the tested range of stresses, the creep experiments have shown that the confining pressure (0-6MPa) did not induce any significant change in creep properties of the intact rock samples. In contrast, the creep curves showed that the fractured samples experienced larger variation in stain which is clearly influenced by the variation of confining pressure. A possible explanation for this might be that the confinement plays an important role in closing up the rock joints and stiffening up the fractured rock specimens.

It is anticipated that in the fractured rock samples the time-dependent process is largely influenced by the shape of fracture and degree of fragmentation. However, in this study, no

systematic investigation was carried out to assess this information. Moreover, the experiments would have benefited from measuring the volumetric and lateral strain.

The data of the creep experiments conducted under various deviatoric stresses was successfully fitted to Burgers model, adopting elasto-viscoplastic properties. In comparison with the intact rock, creep parameters for the fractured rock were found to be significantly smaller, corresponding to the larger creep deformation and the larger steady-state creep rate experienced by the fractured rock samples. Despite this difference between the intact and fractured rock samples, the study showed a considerable correlation between the creep parameters of both types of rock samples and their instantaneous elastic modulus (obtained at typical confining pressures). Regression analysis revealed that creep parameters (of the Burgers model) could be reasonably estimated from instantaneous elastic modulus using an exponential function.

These findings may be somewhat limited by the type of rock, the scale effect due to the small size of the rock samples, and the range of stress level; nevertheless the findings have important implications for setting up a new framework for estimating time-dependent properties of rocks based on their instantaneous (short-term) properties.

A number of possible future studies on another type of rocks using similar experimental approach (however with a wider range of confining pressures and deviatoric stresses, and larger scale of samples to improve the rock mass representation) are apparent. A natural progression of this work is to implement the results into a numerical modelling commercial package and validate the model against a case study. This would be an essential area for improving the geomechanical modelling of long-term stability of abandoned mines as well as for the application of underground disposal of radioactive waste and oil and gas storage.

5 Acknowledgements

The experiments were conducted in the rock mechanics laboratory of Nottingham Centre for Geomechanics (NCG) as part of a research project funded through the Research Programme of the Research Fund for Coal and Steel [grant numbers RFCR-CT-2003-00011].

References

1. Kaiser PK, Morgenstein NR. Time-dependent deformation of small tunnels- I. Experimental facilities. In: *International Journal of Rock Mechanics and Mining Sciences & Geomechanics Abstracts*. Vol 18. ; 1981:129-140.
2. Singh DP. A study of creep of rocks. In: *International Journal of Rock Mechanics and Mining Sciences & Geomechanics Abstracts*. Vol 12. ; 1975:271-276.
3. Liu ZB, Xie SY, Shao J-F, Conil N. Effects of deviatoric stress and structural anisotropy on compressive creep behavior of a clayey rock. *Appl Clay Sci*. 2015;114:491-496.
4. Isherwood D. *Geoscience Data Base Handbook for Modeling a Nuclear Waste Repository*.; 1980.
5. Majer EL, Myer LR, Peterson Jr JE, et al. *Joint Seismic, Hydrogeological, and Geomechanical Investigations of a Fracture Zone in the Grimsel Rock Laboratory, Switzerland*.; 1990.
6. Bieniawski ZT. Time-dependent behaviour of fractured rock. *Rock Mech*. 1970;2(3):123-137.
7. Haramy KY, McDonnell JP. *Causes and Control of Coal Mine Bumps*. US Department of the Interior, Bureau of Mines; 1988.
8. Jeremic ML. Strata mechanics of hydraulic sub-level coal mining. In: *International Journal of*

Rock Mechanics and Mining Sciences & Geomechanics Abstracts. Vol 19. ; 1982:135-142.

9. Wang C, Wang Y, Lu S. Deformational behaviour of roadways in soft rocks in underground coal mines and principles for stability control. *Int J Rock Mech Min Sci*. 2000;37(6):937-946.
10. Jeremic ML. Ground mechanics in hard rock mining. 1986.
11. Munson DE, Dawson PR. *Constitutive Model for the Low Temperature Creep of Salt (with Application to WIPP)*; 1979.
12. Günther R-M, Salzer K, Popp T, Lüdeling C. Steady-state creep of rock salt: improved approaches for lab determination and modelling. *Rock Mech Rock Eng*. 2015;48(6):2603-2613.
13. Challamel N, Lanos C, Casandjian C. Creep damage modelling for quasi-brittle materials. *Eur J Mech*. 2005;24(4):593-613.
14. Cristescu N. *Rock Rheology*. Vol 7. Springer Science & Business Media; 2012.
15. Phillips DW. The nature and physical properties of some coal-measure strata. *Trans Inst Min Eng*. 1931;80(Part 4):212-239.
16. Phillips DW. Further Investigation of the Physical Properties of Coal Measure Rocks and Experimental Work on the Development of Fractures. *Trans*. 1931.
17. Pomeroy CD. Creep in coal at room temperature. *Nature*. 1956;178:279-280.
18. Valsangkar AJ, Gokhale K. Stress-strain relationship for empirical equations of creep in rocks. *Eng Geol*. 1972;6(1):49-53.
19. Larson MK, Wade RG. Creep along weak planes in roof a, nd how it affects stability. 2001.
20. Höwing K, Kutter H. Time-dependent shear deformation of filled rock joints. In: *A Keynote Lecture. Fundamentals of Rock Joints: Proceedings of the International Symposium on Fundamentals of Rock Joints,*. ; 1985:15-20.
21. Wawersik WR. Time-dependent behaviour of rock in compression. In: *Advances in Rock Mechanics: Proceedings of the Third Congress of the International Society for Rock Mechanics, Denver, Colorado*. ; 1974:1-7.
22. Boukharov GN, Chanda MW, Boukharov NG. The three processes of brittle crystalline rock creep. In: *International Journal of Rock Mechanics and Mining Sciences & Geomechanics Abstracts*. Vol 32. ; 1995:325-335.
23. Lu Y, Elsworth D, Wang L. A dual-scale approach to model time-dependent deformation, creep and fracturing of brittle rocks. *Comput Geotech*. 2014;60:61-76.
24. Hamza O, Stace R, Reddish D. A study of the effect of strain rate on stiffness and strength in silty mudstone using multistage triaxial testing. *Post-Mining 2005*. 2005:16-17.
25. Hobbs DW. The behavior oof broken rock under triaxial compression. In: *International Journal of Rock Mechanics and Mining Sciences & Geomechanics Abstracts*. Vol 7. ; 1970:125-148.
26. Yang C, Daemen JJK, Yin J-H. Experimental investigation of creep behavior of salt rock. *Int J Rock Mech Min Sci*. 1999;36(2):233-242.
27. Cristescu N, Hunsche U. *Time Effects in Rock Mechanics*. Wiley New York; 1998.
28. Chan KS, Bodner SR, Fossum AF, Munson DE. A damage mechanics treatment of creep failure in rock salt. *Int J Damage Mech*. 1997;6(2):121-152.
29. Zhang Y, Xu W, Shao J, Zhao H, Wang W. Experimental investigation of creep behavior of clastic rock in Xiangjiaba Hydropower Project. *Water Sci Eng*. 2015;8(1):55-62.
30. Zhang Y, Shao J, Xu W, Jia Y. Time-dependent behavior of cataclastic rocks in a multi-loading triaxial creep test. *Rock Mech Rock Eng*. 2016;49(9):3793-3803.
31. LI Y, YU H, LIU H. Study of creep constitutive model of silty mudstone under triaxial

compression. *Rock Soil Mech*. 2012;7:19.

32. Nomikos P, Rahmannejad R, Sofianos A. Supported axisymmetric tunnels within linear viscoelastic Burgers rocks. *Rock Mech rock Eng*. 2011;44(5):553-564.

33. Parsons RC, Hedley DGF. The analysis of the viscous property of rocks for classification. In: *International Journal of Rock Mechanics and Mining Sciences & Geomechanics Abstracts*. Vol 3. ; 1966:325-335.

34. Zhao Y, Cao P, Wen Y, WANG Y, CHAI H. Elastovisco-plastic rheological experiment and nonlinear rheological model of rocks [J]. *Chinese J Rock Mech Eng*. 2008;3:6.

35. Hardy Jr HR, Kim RY, Stefanko R, Wang YJ, others. Creep and microseismic activity in geologic materials. In: *The 11th US Symposium on Rock Mechanics (USRMS)*. ; 1969.

36. Chin H-P, Rogers JD. Creep parameters of rocks on an engineering scale. *Rock Mech rock Eng*. 1987;20(2):137-146.

37. Hardy HR, others. Time-dependent deformation and failure of geologic materials. In: *The 3rd US Symposium on Rock Mechanics (USRMS)*. ; 1959.

Figure captions:

Fig. 1. Common classified behaviours of rock mass.

Fig. 2. General components of deformation of underground roadways.

Fig. 3. Axial and volumetric strain curves for Lea Hall Sandstone under 35.8 MPa uniaxial stress showing three stages of creep (after Hobbs, 1970).

Fig. 4. Samples of the muddy siltstone: (a) Intact, (b) Fractured.

Fig. 5. Testing Rig with servo-controlled hydraulic pressure cell system used for conducting the creep tests.

Fig. 6. Uniaxial creep test showing the period required to obtain secondary creep in an intact muddy siltstone sample under an axial stress of 32 MPa.

Fig. 7. Four-stage triaxial compression test conducted on an intact sample of muddy siltstone at different confining pressures (σ_3).

Fig. 8. Instantaneous properties: peak strength and elastic modulus of the intact and fractured rock samples

Fig. 9. Creep strain vs. time obtained from (a) four *intact* samples, and (b) four *fractured* samples of the muddy siltstone.

Fig. 10. Strain value (recorded after approximately two days from the start of each loading stage) plotted against deviatoric stress for: (a) Intact rock samples, (b) Fractured rock samples.

Fig. 11. The effect of confining pressure and deviatoric stress on steady state (SS) creep rate in the fractured rock samples.

Fig. 12. Relationship between steady state (SS) strain rate and deviatoric stress for the fractured rock samples.

Fig. 13. Parameters of Burgers model at different confining pressures: (a) Intact rock samples, (b) Fractured rock samples.

Fig. 14. Parameters of Burgers model normalised by the elastic modulus, E: (a) Intact rock samples, (b) Fractured rock samples.

Fig. 15. The exponential relationship between Burgers parameters and short-term elastic modulus (E): (a) Intact rock samples, (b) Fractured rock samples.